SOFT X-RAY EMISSIONS FROM PLANETS AND MOONS

A. Bhardwaj(1), G. R. Gladstone(2), R. F. Elsner(3), J. H. Waite, Jr.(4), D. Grodent(5), T. E. Cravens(6), R. R. Howell(7), A. E. Metzger(8), N. Ostgaard(9), A. Maurellis(10), R. E. Johnson(11), M. C. Weisskopf(3), T. Majeed(4), P. G. Ford(12), A. F. Tennant(3), J. T. Clarke(13), W. S. Lewis(2), K. C. Hurley(9), F. J. Crary(4), E. D. Feigelson(14), G. P. Garmire(14), D. T. Young(4), M. K. Dougherty(15), S. A. Espinosa(16), J.-M. Jahn(2)

(1)*Space Physics Laboratory, Vikram Sarabhai Space Centre, Trivandrum 695022, India, spl_vssc@vssc.org*
(2)*Southwest Research Institute, San Antonio TX 78228, USA*
(3)*NASA Marshall Space Flight Center, Huntsville AL 35812, USA*
(4)*University of Michigan, Ann Arbor MI 48109, USA*
(5)*LPAP, University of Liege, Belgium*
(6)*University of Kansas, Lawrence KS 66045, USA*
(7)*University of Wyoming, Laramie, WY 82071, USA*
(8)*Jet Propulsion Laboratory, Pasadena, CA 91109, USA*
(9)*University of California at Berkeley, Berkeley, CA 94720, USA*
(10)*SRON National Institute for Space Research, Utrecht, The Netherlands*
(11)*University of Virginia, Charlottesville, VA 22903, USA*
(12)*Massachusetts Institute of Technology, Cambridge, MA 02139, USA*
(13)*Boston University, Boston MA 02215, USA*
(14)*Pennsylvania State University, State College, PA 16802, USA*
(15)*Blackett Laboratory, Imperial College, London, England*
(16)*Max-Planck-Institut für Aeronomie, Katlenburg-Lindau, Germany*

ABSTRACT

A wide variety of solar system planetary bodies are now known to radiate in the soft x-ray energy (<5 keV) regime. These include planets (Earth, Jupiter, Venus, Saturn): bodies having thick atmosphere and with/without intrinsic magnetic field; planetary satellites (Moon, Io, Europa, Ganymede): bodies with no/thin atmosphere; and comets and Io plasma torus: bodies having extended tenuous atmosphere. Several different mechanisms have been proposed to explain the generation of soft x-rays from these objects, whereas in the hard x-ray energy range (>10 keV) x-rays mainly result from electron bremsstrahlung process. In this paper we present a brief review of the x-ray observations on each of the planetary bodies and discuss their characteristics and proposed source mechanisms.

1. INTRODUCTION

The energy range of x-ray photons typically spans 0.1-100 keV. Of this wide energy extent the soft x-ray energy band (<5 keV) is an important spectral regime for planetary remote sensing, as a large number of solar system objects are now known to shine at these wavelengths. These include Earth, Moon, Jupiter, Saturn, comets, Venus, Galilean satellites, Mars, Io plasma torus, and the Sun.

Since Earth's thick atmosphere efficiently absorbs x-ray radiation at lower altitudes (<30 km, even for hard x-rays), x-rays can only be observed from space by high-altitude balloons-, rockets-, and satellites-based instruments. But to observe most of the soft x-ray band one has to be above ~100 km from Earth's surface.

Terrestrial x-rays were discovered in the 1950s. The launch of first x-ray satellite UHURU in 1970 marked the beginning of satellite-based x-ray astronomy. Subsequent launch of x-ray observatories - Einstein, and particularly Rontgensatellit (ROSAT), made an important contribution to the planetary x-ray studies. With the advent of sophisticated x-ray observatories - Chandra and XMM-Newton, the field of planetary x-ray astronomy is advancing at a much faster pace.

Earth and Jupiter, as magnetic planets, are observed to emanate strong x-ray emissions from their auroral (polar) regions, thus providing vital information on the nature of precipitating particles and their energization processes in planetary magnetospheres [1,2,3]. X-rays from low latitudes have also been observed on these planets. Saturn should also produce x-rays in the same way as Jupiter, although the intensity is expected to be weaker. Lunar x-rays have been observed from the sunlit hemisphere; a small fraction of dayside x-rays are also seen from the Moon's nightside [4]. Cometary x-rays are now a well-established phenomena; more than a dozen comets have been observed at soft x-ray energies [5,6].

The Chandra X-ray Observatory (CXO) has recently captured soft x-rays from Venus [7,8]. Martian x-rays are expected to be similar to those on Venus. More recently, using CXO [9] have discovered soft x-rays from the inner moons of Jupiter - Io, Europa, and probably Ganymede. The Io Plasma Torus (IPT) is also discovered recently by CXO to be a source of soft x-rays [9]. High spatial resolution observations of Jovian x-rays by CXO/HRC-I have recently revealed a mysterious pulsating (period ~45 minutes) x-ray hot spot in the northern polar regions of Jupiter that have called into question our understanding of Jovian auroral x-rays [10].

In this paper we will present an overview of the x-ray observations on planets, comets, and moons, and discuss the proposed emission production mechanisms.

2. EARTH

Auroral Emissions

Precipitating particles deposit their energy into the Earth's atmosphere by ionization, excitation, dissociation, and heating of the neutral gas. High-energy electrons or ions impacting the nucleus of atoms or molecules can lead to an emission of an x-ray photon by bremsstrahlung with an energy comparable to the energy of the incident particle. The x-ray bremsstrahlung production efficiency is proportional to $1/m^2$, where m is the mass of the precipitating particle. This implies that electrons are 10^6 times more efficient than protons to produce x-ray bremsstrahlung. The production efficiency is a non-linear function of energy, with increasing efficiency for increasing incident energies. For example, for a 200 keV electron the probability of producing an x-ray photon at any energy below 200 keV is 0.5%, while the probability for a 20 keV electron to produce an x-ray photon below 20 keV is only 0.0057% [11].

The main x-rays production mechanism in Earth's auroral zones is bremsstrahlung and therefore the x-ray spectrum of an aurora has been found to be very useful in studying the characteristics of energetic electron precipitation. [12,13,14]. Since the x-ray measurements are not contaminated by sunlight, the remote sensing of x-rays can be used to study energetic electron precipitation on the dayside as well as on the nightside of the Earth [15]. Characteristic line emissions for the main species of the Earth's atmosphere, Nitrogen (K_α at 0.393 keV), Oxygen (K_α at 0.524 keV) and Argon (K_α at 2.958 keV, K_β at 3.191 keV) will also be produced by both electrons and protons, but so far no x-ray observations have been made at energies where these lines are dominant compared to the x-ray bremsstrahlung.

X-ray photons from bremsstrahlung are emitted dominantly in the direction of the precipitating electron velocity. Consequently, the majority of the x-ray photons in Earth's aurora are directed towards the planet. These downward propagating x-rays, therefore, cause additional ionization and excitation in the atmosphere below the altitude where the precipitating particles have their peak energy deposition [e.g., 16,17]. A fraction of the x-ray emission that is moving away from the ground can be used to study the x-rays from satellite-based x-ray imagers, e.g, AXIS on UARS and PIXIE on POLAR.

Auroral x-ray bremsstrahlung has been observed from balloons and rockets since 1960s and from spacecraft since the 1970s [18,19,20,13]. Due to detector techniques that have been used, only x-rays above ~3 keV have been observed from the Earth's ionosphere. The PIXIE (Polar ionospheric X-Ray Imaging Experiment) aboard Polar is the first x-ray detector that provides true 2-d global x-ray image ta energies >~3 keV [21]. Because of the high apogee of Polar satellite (~9 R_E), PIXIE is able to image the entire auroral oval with a spatial resolution of ~700 km for long duration when the satellite is around apogee. This has helped to study the morphology of x-ray aurora and its spatial and temporal variation, and consequently the evolution of energetic electron precipitation during magnetic storms (days) and substorms (1-2 hours). Based on data from the PIXIE camera, [22] showed that the x-ray substorm brightens up in the midnight sector and has a prolonged and delayed maximum in the morning sector due to the scattering of drifting electrons. Statistically the x-ray bremsstrahlung intensity peaks in the midnight substorm onset, is significant in the morning sector and has a void in the early dusk sector [23]. During the onset/expansion phase of a typical substorm the electron energy deposition rate is 60-90 GW, which produces 10-30 MW bremsstrahlung x-rays [24]. Combining the results of PIXIE with UV imager aboard Polar it is now possible to derive the energy distribution of precipitating electrons in the 0.1-100 keV range [14].

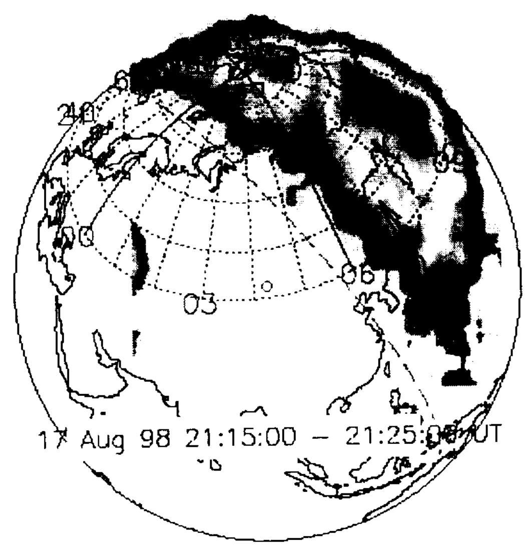

Fig.X1. X-ray image of Earth from the Polar PIXIE instrument for energy range 2.9-10.1 keV.

Non-Auroral

{ - Incomplete}

.....The non-auroral background x rays above 2 keV from the Earth is almost completely negligible except for brief periods during major solar flares [23]. During flares, solar x-rays light up the sunlit side of the Earth by Thomson scattering, as well as by fluorescence of atmospheric argon to produce characteristic x-rays at 3 keV. The x-ray brightness can be comparable to that of a moderate aurora [23]. Although the fluxes were slightly larger than expected from NOAA GOES measurements they showed that the shape of the measured x ray spectra was in fairly good agreement with modeled spectra of solar x-rays subject to Thomsen scattering in the Earth's atmosphere.......

3. JUPITER

Auroral Emissions

The first detection of x-ray emissions from Jupiter was made by the satellite-based Einstein observatory in 1979 [25]. The emissions were detected in the 0.2-3.0 keV energy range from both poles of Jupiter. Analogous to the processes on Earth, it was expected that Jupiter's x-rays might originate as bremsstrahlung by precipitating electrons [26]. However, the power requirement for producing the observed emission with this mechanism (10^{15}-10^{16} W) is more than two orders of magnitude larger than the input auroral power available as derived from Voyager and IUE observations of the ultraviolet aurora [cf.2]. Ref. [25] suggested a mechanism implying K-shell line emissions from precipitating energetic sulfur and oxygen ions from the inner magnetosphere, with energies in the 0.3-4.0 MeV/nucleon range. The heavy ions are thought to emit x-rays by first charge stripping to a highly ionized state, followed by charge exchange and excitation through collisions with H_2. The bremsstrahlung process was further ruled out by theoretical models [27,28] showing that primary and secondary precipitating electrons in the 10-100 keV energy range are inefficient at producing the observed x-ray emissions.

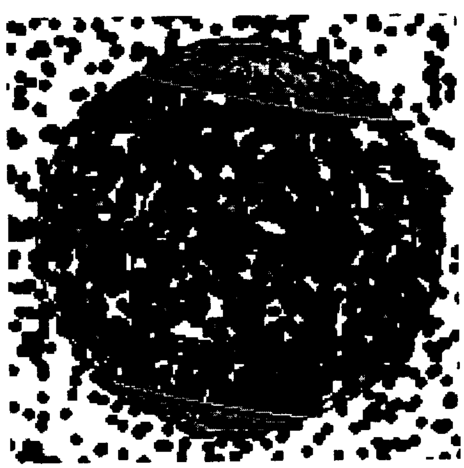

Fig. X1. CXO image of Jupiter on 18 December 2000. [from Ref. 10].

Furthermore, during its Jovian flyby, the Ulysses spacecraft did not detect significant emissions in the 27-48 keV energy range [29] as would have been the case if electron bremsstrahlung was a major process. Observations of Jupiter x-ray's emissions by ROSAT [30] supported the suggestion of [25] and the model calculations [27,28] that precipitating energetic (>700 keV per nucleon) S and O ions are most probably responsible for the x-ray emissions from Jupiter. A detailed modeling of the x-ray production [31,32] suggests that recombination lines from highly charged precipitating O and S ions mainly contribute to the soft x-rays detected by ROSAT. Recent high-spatial resolution observations of Jupiter with the Chandra telescope [10] reveal that most of Jupiter's northern auroral x-rays come from a "hot spot" located significantly poleward of the latitudes connected to the inner magnetosphere. The hot spot is fixed in magnetic latitude and longitude and occurs in a region where anomalous infrared and ultraviolet emissions (the so called "flares") have also been observed. Its location must connect along magnetic field lines to regions in the Jovian magnetosphere well in excess of 30 Jovian radii from the planet, a region where there are insufficient S and O ions to account for the hot spot [10]. More surprising, the hot spot x-rays pulsate with an approximately 45-min period, similar to that reported for high-latitude radio and energetic electron bursts observed by near-Jupiter spacecraft. These results invalidate the idea that Jovian auroral x-ray emissions are mainly excited by steady precipitation of heavy energetic ions from the inner magnetosphere. Instead, the x-rays seem to result from currently unexplained processes in the outer magnetosphere that produce highly localized and highly variable emissions over an extremely wide range of wavelengths. In any case the power needed to produce the brightest ultraviolet "flares" seen in the same polar cap region as the x-ray hot spot is a few tens of TW, much less than the estimated power of a few PW needed to produce the observed x-rays by electron bremsstrahlung. Thus, electron bremsstrahlung still seems to fail in explaining the observed Jovian x-rays hot-spot. One possible source of Jovian x-rays production is via charge-exchange of solar wind ions that penetrate down the atmosphere in the magnetic cusp region. But in this case the solar wind ions would have to be accelerated to much higher energies (100s of keV), probably by parallel electric field or wave particle interactions, to generate sufficient luminosity to account for the observations. In summary, at the present time the origin of the Jovian x-rays and its source is still an open issue.

Non-Auroral Emissions

Soft x-ray emissions with brightnesses of about 0.01-0.2 Rayleighs were observed from the equatorial regions of Jupiter using the ROSAT/HRI. It was proposed [33] that the equatorial emission, like the auroral emission, may be largely due to the precipitation of energetic (>300 keV/amu) sulfur or oxygen ions into the atmosphere from the radiation belts. Further evidence for a correlation between regions of low magnetic field strength and enhanced emission [34] lent additional support to this mechanism, since it can be assumed that the loss cone for precipitating particles is wider in regions of weak surface magnetic field. However, [35] showed that two alternative mechanisms should not be overlooked in the search for a complete explanation of low-latitude x-ray emission, namely elastic scattering of solar x-rays by atmospheric neutrals and fluorescent scattering of carbon K-shell x-rays from methane molecules located below the Jovian homopause. Modeled brightnesses agree, up to a factor of two, with the bulk of low-latitude ROSAT/PSPC measurements which suggests that solar photon scattering (~90% elastic scattering) may act in conjunction with energetic heavy ion precipitation to generate Jovian non-auroral x-ray emission. Solar x-ray scattering mechanism is also suggested from the correlations of Jovian emissions with the F10.7 solar flux and of the x-ray limb with the bright visible limb [34]. Jupiter was observed in December 2000 by Chandra HRC-I, from which disk-averaged emitted x-rays power of about 2 GW was estimated [10], but the coverage of the disk was still not adequate to show the limb brightening expected by solar photon-driven x-ray emission.

4. MOON

Though being the Earth's nearest planetary body, the Moon has been relatively little studied at x-ray wavelengths. Other than the discovery observation by [4] using the ROSAT PSPC and a detection by Advanced Satellite for Cosmology and Astrophysics (ASCA) [35], most recent high-energy remote sensing of the Moon has been made at extreme- and far-ultraviolet wavelengths [e.g., 36,37,38]. However, as noted by [39], x-ray fluorescence studies could provide an excellent way to determine the elemental composition of the lunar surface by remote sensing, since the soft x-ray optical properties of the lunar surface should be dominated by elemental abundances (rather than mineral abundances, which determine the optical properties at visible and longer wavelengths). Although reflection of the strong solar lines likely dominates the soft x-ray spectrum of the Moon, the detection of weaker emissions due to L- and M-shell fluorescence would provide a direct measure of specific elemental abundances.

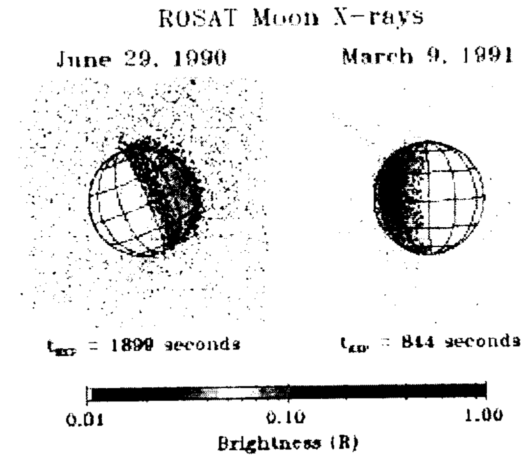

Figure X1. ROSAT soft x-ray (0.1-2 keV) images of the Moon at first (left side) and last (right side) quarter. The dayside lunar emissions are thought to be primarily reflected and fluoresced sunlight, while the origin of the faint but distinct nightside emissions is uncertain. The brightness scale in R assumes an average effective area of 100 cm^2 for the ROSAT PSPC over the lunar spectrum.

Fig. X-1 shows ROSAT data; the left image shows the [4] data, while the right image is unpublished data from a lunar occultation of the bright x-ray source GX5-1 (the higher energy x-rays from GX5-1 have been suppressed in this figure, but a faint trail to the upper left of the Moon remains). The power of the reflected and fluoresced x-rays observed by ROSAT in the 0.1-2 keV range coming from the sunlit surface was determined by [4] to be only 73 kW, making the Moon the faintest x-ray source in the sky (the flux measured was 2.5×10^{12} erg cm^{-2} s^{-1}).

While the dayside lunar soft x-rays are reflected and fluoresced sunlight, the faint but distinct lunar nightside emissions are a matter of controversy. Ref. [4] suggest that solar wind electrons of several hundred eV might be able to impact the night side of the Moon on the leading hemisphere of the Earth-Moon orbit around the sun. However, this was before the GX5-1 data were acquired, which clearly show lunar nightside x-rays from the trailing hemisphere as well. Another possible explanation is the accepted mechanism for comet x-rays, heavy ion solar wind charge exchange (SWCX) [e.g., 6]. In this case, however, the heavy ions in the solar wind would be charge exchanging with geocoronal H atoms that lie between the Earth and Moon but lie outside the Earth's magnetosphere.

Future observations of the Moon's x-rays by Chandra and XMM are likely, and there is a planned x-ray spectrometer D-CIXS on ESA's SMART-1 lunar mission [40] that will provide global coverage of ambient x-ray emission. This will greatly improve upon the elemental abundance maps produced by the x-ray spectrometers on Apollo 15 and 16 [41].

5. COMETS

X-ray emission from a comet was first discovered in 1996 with the ROSAT observations of comet Hyakutake [42]. Extreme ultraviolet (EUV) emission was also detected from this comet by the EUVE satellite [43]. Since the initial discovery of cometary x-ray emission, it has been shown that active comets are almost always EUV and x-ray sources [44]. A thorough review of this topic has just appeared [6], so only a brief summary is provided here.

Fig. X. Left: Images of comet C/LINEAR 1999 S4 from July 2002 obtained by CXO ACIS-S. Right: Visible light image showing a coma and tail. The plus sign mark the position of the nucleus. [from Ref. 5]

The key observational features of cometary x-ray emission are now summarized. The x-ray emission is "very soft" with photon energies of a few hundred eV or less. High-resolution x-ray spectra of comets C/Linear 1999 S4 [5] and McNaught-Hartley (C/1999 T1) [45] have recently been measured by the CXO. Emission lines associated with highly charged ions (in particular, O^{6+}) are evident in these spectra. A spectrum of comet Hyakutake from the EUVE satellite [46] also displays line emission. Cometary x-ray luminosities are quite large and tend to correlate with the gas production rate [e.g., 47]. The comet Hyakutake x-ray luminosity measured by ROSAT was about 1 GW. Cometary x-ray emission is spatially very extensive with observed emission out to radial distances from the cometary nucleus of 10^5-10^6 km [e.g., 5,42] The emission is also time variable and has been shown to correlate with the solar wind flux [e.g., 48].

Several cometary x-ray emission mechanisms were proposed following the initial discovery. These include bremsstrahlung associated with solar wind electron collisions with cometary neutrals and ions, K-shell ionization of neutrals by electron impact, scattering of solar photons by cometary dust, and charge transfer of solar wind heavy ions with neutrals [cf. 6]. The SWCX mechanism [49] has gradually won favor. In this mechanism highly charged solar wind ions (e.g., O^{6+}, O^{7+}, C^{6+}, Ne^{9+},...) undergo charge transfer collisions when they encounter cometary neutrals. The product ions are invariably left in highly excited states and emit EUV and soft x-ray photons. This mechanism is able to explain the luminosity, spatial distribution [50], time variability [48], and spectrum [5,45,51,52] of the x-ray emission.

6. VENUS

In January 2001 the CXO discovered soft x-ray emissions from Venus [7,8]. Observations were performed with the CXO's ACIS-I high-resolution imaging camera and with the LETG/ACIS-S high-resolution grating spectrometer. The x-ray emission originated on the sunlit hemisphere, exhibited noticeable limb brightening (when compared to visible disk), and consisted primarily of O-K-alpha at ~530 eV. The C-K-alpha line emission at ~280 eV was also detected, with marginal evidence for N-K-alpha emission at ~400 eV. The carbon emission might also include a 290 eV line from CO_2 and CO. The derived energy fluxes in the oxygen and carbon lines were $\sim 20 \times 10^{-14}$ erg cm^{-2} s^{-1} for O-K-alpha and $\sim 5 \times 10^{-14}$ erg cm^{-2} s^{-1} for C-K-alpha. The total power in Venusian x-rays was estimated to be 30-70 MW. The Chandra data also indicated possible time variability on a timescale of a few minutes.

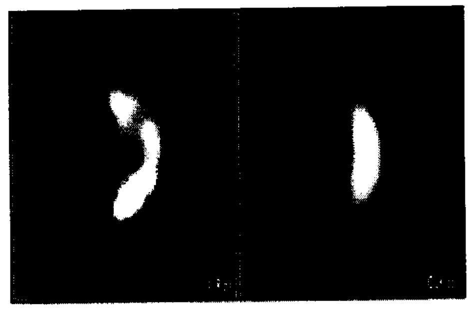

Fig. X1. X-ray image of Venus obtained with Chandra ACIS-I on 13 January 2001. Right is an optical image of Venus. [from Ref. 8].

The observers argue persuasively that the x-ray emission from Venus results from fluorescent scattering of solar x-rays, as predicted by [53], and not from charge exchange between heavy ions in the solar wind and neutral atoms in the Venusian atmosphere. Their detailed modeling of the interaction between solar x-rays and the planetary atmosphere showed that the fluorescent scattering occurred ~110 km or higher above the planet's surface. The amount of limb brightening predicted by their models depended sensitively on the chemical composition and the density profile in Venus's upper atmosphere.

7. GALILEAN SATELLITES

Recently the CXO has discovered x-ray emission from the Galilean satellites [9]. The CXO observations of the Jovian system were made on 25-26 November 1999 for 86.4 ks with the ACIS-S instrument and on 18 December 2000 for 36.0 ks with the HRC-I instruments. The time tagged nature of the CXO data makes it possible to correct for varying satellite motions, and with ACIS it is also possible to filter the data by energy for optimum sensitivity. During the ACIS-S observation, Io and Europa were detected with a high degree of confidence, and Ganymede at a lesser degree of confidence. Io was also detected with high confidence during the shorter HRC-I observation. Over the nominal energies of 300-1890 eV range detected by ACIS-S, the x-ray events show a clustering between 500 and 700 eV, probably dominated by the oxygen K-alpha line at 525 eV. The nominal energies of the x-ray events cluster between 500 and 700 eV, suggestive of oxygen K-alpha line emission at 525 eV. The estimated energy fluxes at the telescope and power emitted are 4×10^{-16} erg cm^{-2} s^{-1} and 2.0 MW for Io, and 3×10^{-16} erg cm^{-2} s^{-1} and 1.5 MW for Europa. Ganymede was roughly a third as luminous as Io. Callisto was not detected in either set of data.

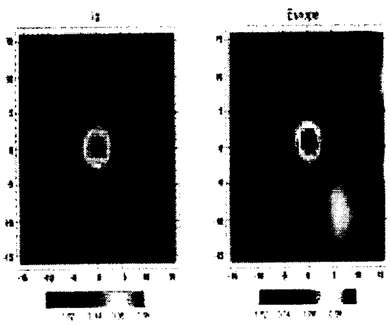

Fig. X1. Chandra ACIS-I image (0.2-2 keV) of Io and Europa obtained on Nov 25-26, 1999. The solid circle shows the size of the satellite (the radii of Io and Europa are 1821 km and 1560 km, respectively), and the dotted circle the size of the detect cell. The axes are labeled in arcsec (1 arcsec ≈ 2995 km) and the scale bar is in units of smoothed counts per image pixel (0.492 by 0.492 arcsec). [from Ref 9].

The most plausible emission mechanism is inner (K shell) ionization of the surface (and perhaps incoming magnetospheric) atoms followed by prompt x-ray emission. Oxygen should be the dominant emitting atom in either a silicate or SO2 surface (Io) or in an icy one (the outer Galilean satellites). It is also the most common heavy ion in the magnetosphere. The extremely tenuous atmospheres of the satellites are transparent to x-ray photons with these energies, and also to much of the energy range of the incoming ions. However oxygen absorption of the 525 eV line is such that the x-rays must originate in the top ~10 microns of the surface in order to escape. Simple estimates suggest that excitation by incoming ions dominates over electrons and that the x-ray flux produced is sufficient to account for the observations. Detailed models are required for verifying this picture and also for predicting the strengths of K-alpha lines for elements other than oxygen, especially heavier ones such as Na, Mg, Al, Si, and S. Within this framework, it is in principle possible to constrain the surface composition of these moons from x-ray observations, but this requires greater sensitivity than provided by the Chandra observations. The detection of x-ray emission from the Galilean satellites thus provides a direct measure of the interactions of magnetosphere of Jupiter with the satellite surfaces.

8. IO PLASMA TORUS

The Io Plasma Torus (IPT) is known to emit at EUV energies and below [54,55,56], but it was a surprise when CXO discovered that it was also a soft x-ray source [9]. The Jovian system has so far been observed with Chandra using the ACIS-S high-spatial-resolution imaging camera, which also has modest energy resolution, for two Jovian rotations in November 1999, and using the HRC-I high-spatial-resolution camera, with essentially no energy resolution, for one rotation in December 2000. X-ray emission from the IPT is present in both observations. The ACIS-S spectrum was consistent with a steep power-law continuum (photon index 6.8) plus a gaussian line (complex) centered at ~569 eV, consistent with K-alpha emission from various charge species of oxygen. Essentially no x-rays were observed above this spectral feature, consistent with the steepness of the power-law continuum. The 250-1000 eV energy flux at the telescope aperture was 2.4×10^{-14} erg cm^{-2} s^{-1}, corresponding to a luminosity of 0.12 GW, and was approximately evenly divided between the dawn and dusk side of Jupiter. However, the line emission originated predominantly on the dawn side. During the ACIS-S observation, Io, Europa, and Ganymede were on the dawn side, while Callisto was on the dusk side. For the HRC-I observation, the x-ray emission was stronger on the dusk side, approximately twice that observed on the dawn side. During the HRC-I observation, Io, Europa, and Ganymede were on the dusk side, while Callisto was on the dawn side.

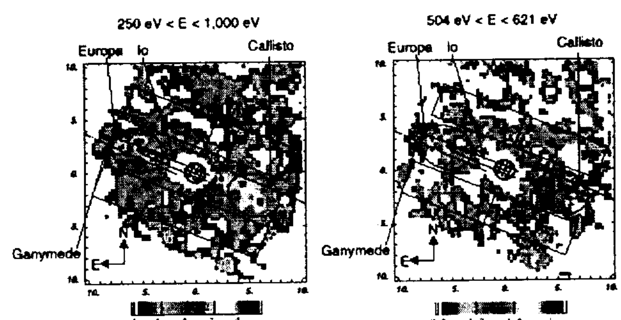

Fig.X1. Chandra ACIS-I image of Io plasma torus obtained on Nov. 25-26, 1999. The axes are labelled in units of Jupiter's radius, R_J and the scale bar is in units of smoothed counts per image pixel (7.38 by 7.38 arcsec). For this observation, Jupiter's radius corresponds to 23.8 arcsec. The paths traced by Io (solid line to the east), Europa (dashed line), Ganymede (dotted line), and Callisto (solid line to the west) are marked on the image. The regions bounded by rectangles were used to determine background. The regions bounded by ellipses were defined as source regions. [from Ref. 9].

The physical origin of the x-ray emission from the IPT is not yet fully understood. According to the estimates given in [9], fluorescent x-ray emission excited by solar x-rays, even during flares from the active Sun, charge-exchange processes, previously invoked to explain Jupiter's x-ray aurora [e.g., 2,31] and cometary x-ray emission [e.g., 6,49], and ion stripping by dust grains fail to account for the observed emission. Assuming bremsstrahlung emission of soft X-rays by non-thermal electrons in the few hundred to few thousand eV range, with a kappa, or generalized Lorentzian, distribution with a temperature of 10 eV and an index of $\kappa = 2.4$ [57], which is consistent with the in-situ Ulysses observations, [9] estimated an IPT soft x-ray luminosity of 0.03 GW. This falls short of but is a significant fraction of the observed luminosity of 0.12 GW.

9. MARS

There seems to be a tentative detection of Martian x-rays in the ROSAT data [58]. However, so far no x-ray emission has been unambiguously detected from Mars, but this situation is expected to change soon. Alike at Venus, absorption of solar x-rays in either the carbon or oxygen K-shells followed by fluorescent emission of x-rays is suggested as the dominant process of x-rays production on Mars [53]. The predicted total soft x-ray intensity is 0.15 R that corresponds to x-ray luminosity of about 2.5 MW [53], which exceed the x-ray luminosity expected from the solar wind charge exchange mechanism on Mars [59]. A simulated image of SWCX-produced x-ray emission at Mars [59] indicates that this emission has a very different spatial morphology than the fluoresce x-ray emission [53], and future observations must be able to distinguish between the two processes.

10. SATURN

{Incomplete}
.....Saturn is expected to have a predominantly solar-driven elastic scattering component to its x-ray radiation, much like Jupiter (predominantly H_2 scattering with a small CH_4 component) with perhaps about a third as much integrated non-auroral power as Jupiter.....

11. SUMMARY

Table 1 summaries our current knowledge of the x-ray emissions from the planetary bodies that have been observed to produce soft x-rays.

The x-rays from solar system bodies are relatively too weak (< few GW) and are from a much cold ($T < 10^3$ K) environment compared to the x-rays from stars and other cosmic bodies (>TW, $T > 10^6$ K). Nonetheless, the studies of planetary x-rays help advance our understanding of basic plasma-neutral (in both gas and solid phase) interactions that are important within our solar system, and plausibly in the extra-solar planetary systems as well.

12. REFERENCES

1. Robinson, R.M., and Vondark, R.R., Validation techniques for space based remote sensing of auroral precipitation and its ionospheric effects, *Space Sci. Rev.*, 69, 331, 1994.

2. Bhardwaj, A. and Gladstone, G. R. Auroral emissions of the giant planet, *Rev. Geophys.*, 38, 295-353, 2000.

3. Waite, J.H., Jr., and Lummerzheim D., Comparison of auroral processes: Earth and Jupiter, in *Atmospheres in the Solar System: Comparative Aeronomy*, AGU Geophysical Monograph 130, p.115-139, AGU, Washington DC, 2002.

4. Schmitt, J. H. M. M., Snowden S. L., Aschenbach B., Hasinger G., Pfeffermann E., Predehl P., and Trumper J., A soft x-ray image of the moon, *Nature*, 349, 583-587, 1991.

5. Lisse, C. M. et al., Charge exchange-induced x-ray emission from comet C/1999 S4 (LINEAR), *Science*, 292, 1343, 2001.

6. Cravens, T. E., X-ray emission from comets, Science, 296, 1042, 2002.

7. Dennerl, K., Burwitz, V., Englhauser, J., Lisse, C., and Wolk, S.,The discovery of x-rays from Venus with Chandra, in *Proc. Symposium "New Visions of the X-ray Universe in the XMM-Newton and Chandra Era"*, ESA SP-488, eds. F. Jansen et al., 2002.

8. Dennerl, K., Burwitz, V., Englhauser, J., Lisse, C., and Wolk, S.,Discovery of x-rays from Venus with Chandra, *Astron. Astrophys.*, 386, 319-330, 2002.

9. Elsner, R.F., et al. Discovery of soft x-ray emission from Io, Europa, and Io plasma torus, *Astrophys. J.*, 572, 1077-1082, 2002.

10. Gladstone, G.R., Waite J. H., Jr, Grodent D, Lewis W. S., Crary F. J., Elsner R. F., Weisskopf M. C., Majeed T., Jahn J.-M., Bhardwaj A., Clarke J. T., Young D. T., Dougherty M. K., Espinosa S. A., Cravens T. E., A pulsating auroral X-ray hot spot on Jupiter, *Nature*,415, 1000-1003, 2002.

11. Berger, M. J. and Seltzer, S. M., Bremsstrahlung in the Atmosphere, *J. Atmos. Terr. Phys.*, 34, 85, 1972.

12. Vij, K.K., et al., Simultaneous investigation of parent electrons and bremsstrahlung x-rays by rocket-borne detectors, *J. Geophys. Res.*, 80, 2869, 1975.

13. Stadsnes J., Aarsnes K., and Bjordal J., *Adv. Space Res.*, 20, No.4/5, 1043-1054, 1997.

14. N. Ostgaard, et al., Auroral electron distributions derived from combined UV and x-ray emissions, J. Geophys. Res, 106, 26081-26089, 2001.

15. Petrinec, S.M., et al., Dayside/nightside auroral x ray emission difference - implications for ionospheric conductance, *Geophys. Res. Lett*, 27, 3277-3279, 2000.

16. Winningham J.D., et al., The UARS Particle Environment Monitor, *J. Geophys. Res.*, 98, 10649, 1993.

17. Sharber J.R., et al., Observations of the UARS particle environment monitor and computation of ionization rates in the middle and upper atmosphere during a geomagnetic storm, *Geophys. Res. Lett.*, 20, 1319, 1993.

18. Anderson, K., Balloon measurements of x-rays in the auroral zone, in *Auroral Phenomena*, ed. M. Walt, pp.46-83, Stanford Univ. Press, Stanford, CA, 1965.

19. Imhof, W.L., Review of energetic (>20 keV) bremsstrahlung x-ray measurements from satellite, *Space Sc. Rev.*, 29, 201-217, 1981.

20. Van Allen J.A., Early rocket observations of auroral bremsstrahlung and its absorption in the mesosphere, *J. Geophys. Res.*, 100, 14485-14497, 1995.

21. Imhof, W.L., et al., The Polar Ionospheric X-ray Imaging Experiment (PIXIE), *Space Sc. Rev.*, 71, 385, 1995

22. Ostgaard N., et al., Global Scale electron precipitation features seen in UV and X-rays during substorms, *J. Geophys. Res*, 104, 10,191-10,204, 1999.

23. Petrinec, S. M., McKenzie D. L., Imhof W. L., Mobilia J. and Chenette D., Studies of X-ray observations from PIXIE, *jatp*, 74, 4687-4693, 1999.

24. Ostgaard N., Germany G. A., Stadsnes J., and Vondrak R. R., Energy analysis of substorms based on remote sensing techniques, solar wind measurements and geomagnetic indices, *J. Geophys. Res*, in press, 2002.

25. Metzger, A. E., Gilman D. A., Luthey J. L., Hurley K. C., Schnopper H. W., Seward F. D., and Sullivan J. D., The detection of X rays from Jupiter, *J. Geophys. Res.*, 88, 7731-7741, 1983.

26. Barbosa, D. D., Bremsstrahlung X-rays from Jovian auroral electrons, *J. Geophys. Res.*, 95, 14,969-14,976, 1990.

27. Waite, J. H., Jr., Comment on "Bremsstrahlung X rays from Jovian auroral electrons" by D. D. Barbosa, *J. Geophys. Res.*, 96, 19,529-19,532, 1991.

28. Singhal, R. P., Chakravarty S. C., Bhardwaj A., and Prasad B., Energetic electron precipitation in Jupiter's upper atmosphere, *J. Geophys. Res.*, 97, 18,245-18,256, 1992.

29. Hurley, K. C., Sommer M., and Waite J. H. Jr., Upper limits to Jovian hard X radiation from the Ulysses gamma ray burst experiment, *J. Geophys. Res.*, 98, 21,217-21,219, 1993.

30. Waite, J. H., Jr., Bagenal F., Seward F., Na C., Gladstone G. R., Cravens T. E., Hurley K. C., Clarke J. T., Elsner R., and Stern S. A., ROSAT observations of the Jupiter aurora, *J. Geophys. Res.*, 99, 14,799-14,809, 1994.

31. Cravens, T. E., Howell E., Waite J. H. Jr., and Gladstone G. R., Auroral oxygen precipitation at Jupiter, *J. Geophys. Res.*, *100*, 17,153-17,161, 1995.

32. Kharchenko, V., Liu W.H., and Dalgarno A., X-ray and EUV emission spectra of oxygen ions precipitating into the Jovian atmosphere, *J. Geophys. Res.*, 103, 26687-26698, 1998.

33. Waite J. H., Gladstone G. R., Lewis W. S., Drossart P., Cravens T. E., Maurellis A. N., Mauk B. H., Miller S., Equatorial X-ray emissions: Implications for Jupiter's High Exospheric Temperatures, *Science*, 276, 104-108, 1997.

34. Gladstone G. R., Waite J. H., Lewis W. S., Secular and local time dependence of Jovian X ray emissions, *J. Geophys. Res.*, 103, 20083-20088, 1998.

35. Maurellis A. N., Cravens T. E., Gladstone G. R., Waite J. H. Jr., and Acton L., Jovian X-ray Emission from Solar X-ray Scattering, *Geophys. Res. Lett*, 27, 1339-1342 2000.

35. Kamata, Y., Takeshima T., Okada T., and Terada K., Detection of x-ray fluorescence line feature from the lunar surface, *Adv. Space Res.*, 23, 1829-1832, 1999.

36. Gladstone, G. R., McDonald J. S., Boyd W. T., and Bowyer S., EUVE photometric observations of the moon, *Geophys. Res. Lett.*, 21, 461-464, 1994.

37. Henry, R. C., Feldman P. D., Kruk J. W., Davidsen A. F., and Durrance S. T., Ultraviolet albedo of the moon with the Hopkins Ultraviolet Telescope, *Astrophys. J.*, 454, L69-L72, 1995.

38. Flynn, B., Vallerga J., Gladstone G. R., and Edelstein J., Lunar reflectivity from Extreme Ultraviolet Explorer imaging and spectroscopy of the full moon, *Geophys. Res. Lett.*, 25, 3253-3256, 1998.

39. Edwards, B. C., Priedhorsky W. C., and Smith B. W., Expected extreme ultraviolet spectrum of the lunar surface, *Geophys. Res. Lett.*, 18, 2161-2164, 1991.

40. Grande, M. et al., The D-CIXS x-ray spectrometer on ESA's SMART-1 mission to the Moon, *Planet. Space Sci.*, in press, 2002.

41. Adler, I., Trombka J., Lowman P., Schmadebeck R., Blodget H., Eller E., Yin L., Gerard J., Gorenstein P., Bjorkholm P., Gursky H., Harris B., and Osswald G., Results of the Apollo 15 and 16 x-ray fluorescence experiment, *Lunar and Planetary Science Conference* (abstract), 4, 9, 1973.

42. Lisse, C. M. et al., Discovery of x-ray and extreme ultraviolet emssion from comet C/Hyakutake 1996 B2, *Science*, 274, 205, 1996.

43. Mumma, M. J., Krasnopolsky V. A., and Abbott M. J., Soft x-rays from four comets observed with EUVE, *Astrophys. J.*, 491, L125, 1997.

44. Dennerl, K., Englhauser J., and Trumper J., X-ray emissions from comets detected in the Roentgen X ray Satellite all-sky survey, *Science*, 277, 1725-1630, 1997.

45. Krasnopolsky, V. A. et al., X-ray emission from comet McNaught-Hartley (C/1999 T1), submitted to *Icarus*, 2002.

46. Krasnopolsky, V. A., and Mumma M. J., Spectroscopy of comet Hyakutake at 80-700 A: First detection of solar wind charge transfer emissions, *Astrophys. J.*, 549, 629, 2001.

47. Lisse, C. M. et al., X-ray and extreme ultraviolet emission from comet P/Encke 1997, *Icarus*, 141, 316, 1999.

48. Neugebauer, M., et al., The relation of temporal variations of soft x-ray emission from comet Hyakatke to variations of ion fluxes in the solar wind, *J. Geophys. Res.*, 105, 20949, 2000.

49. Cravens, T. E., Comet Hyakutake x-ray source: Charge transfer of solar wind heavy ions, *Geophys. Res. Lett.*, 25, 105-109, 1997.

50. Häberli, R. M. et al., Modeling of cometary x-rays caused by solar wind minor ions, *Science*, 276, 939, 1997.

51. Schwadron, N. A. and Cravens T. E., Implications of solar wind composition for cometary x-rays, *Astrophys. J.*, 544, 558, 2000.

52. Kharchenko, V. A., and Dalgarno A., Variability of cometary x-ray emission induced by solar wind ions, *Astrophys. J.*, 554, L99, 2001.

53. Cravens T. E. and Maurellis A. N., X-ray emission at Venus and Mars from solar x-ray scattering and fluorescence, *Geophys. Res. Lett.*, 28, 3043-3046, 2001.

54. Hall, D. T. et al., Extreme Ultraviolet Explorer satellite observation of Jupiter's Io plasma torus, *Astrophys. J.*, 426, L51-L54, 1994.

55. Woodward, R. C., Scherb, F. and Roesler, F. L., *Astrophys. J.*, 479, 984, 1997.

56. Gladstone, G. R. and Hall, D. T. Recent results from EUVE observations of the Io plasma torus, *J. Geophys. Res.*, 103, 19927-19933, 1998

57. Meyer-Vernet, N. Moncuquet, M., and. Hoang, S., *Icarus*, 116, 202, 1995

58. Holmstrom, M., X ray imaging of the interaction between the solar wind and non-magnetized planets, *IRF Sci.Rept. 274*, Swedish Inst. Space Phys., Kiruna, 2001.

59. Holmstrom, M., Barabash, S., and Kallio E., X-ray imaging of the solar wind-Mars interaction, *Geophys. Res. Lett.*, 28, 1287-1290, 2001.

Table 1. Summary of the characteristics of soft x-rays from planets and moons

Object	Emitting Region	Power Emitted[a]	Special Characteristics	Possible Production Mechanism	References[b]
Earth	Auroral atmosphere	10-30 MW	Correlated with substorm activity	Bremsstrahlung from precipitating electrons	Ostgarrd et al. (2002)
Earth	Non-auroral atmosphere	40 MW		Scattering of solar x-rays by atmosphere	Snowden and Freyberg (1993)
Jupiter	Auroral atmosphere	0.4-1 GW	Pulsating (~45 min) x-ray hot spot in North polar region	Energetic ion precipitation from magnetosphere and/or solar wind + electron bremsstrahlung + ?	Metzger etal (1983) Gladstone et al. (2002)
Jupiter	Non-auroral atmosphere	0.5-2 GW	Quite uniform over disk	Resonant scattering of solar x-rays + Ion precipitation from ring current	Waite et al. (1997) Gladstone et al. (2002)
Moon	Surface - Dayside - Nightside	0.07 MW	Nightside emissions are ~1% of the dayside emissions	Scattering of solar x-rays by the surface elements on dayside. Electron bremsstrahlung + SWCX on nightside	Schmitt et al. (1991)
Comets	Sunward-side coma	0.2-1 GW	Intensity peaks in sunward direction ~10^5-10^6 km ahead of cometary nucleus	Charge transfer of heavy highly ionized solar wind ions with cometary neutrals + other mechanisms	Lisse et al. (1996, 2001)
Venus	Sunlit atmosphere	50 MW	Emissions come from ~120-140 km above the surface	Fluorescent scattering of solar x-rays by C and O atoms in atmosphere	Dennerl et al. (2002)
Io	Surface	2 MW	Emissions from upper few microns of the surface	Energetic Jovian magnetospheric ions impact on the surface + ?	Elsner et al. (2002)
Europa	Surface	1.5 MW	Emissions from upper few microns of the surface	Energetic Jovian magnetospheric ions impact on the surface + ?	Elsner et al. (2002)
Io Plasma Torus	Plasma torus	0.1 GW	Dawn-dusk asymmetry observed	Electron bremsstrahlung + ?	Elsner et al. (2002)
Saturn	Auroral and non-auroral atmosphere	0.4 GW	Plausibly similar to Jovian x-rays	Electron bremsstrahlung + scattering of solar x-rays	Ness and Schmitt (2000)
Mars	Atmosphere	3 MW	Probable detection	Solar fluorescence + SWCX	Holmstrom (2001)

[a]The values quoted are "typical" values at the time of observation. X-rays from all bodies are expected to vary with time.
[b]Only representative references are given.
SWCX = Solar wind charge exchange = charge exchange of heavy highly ionized solar wind ions with neutrals.